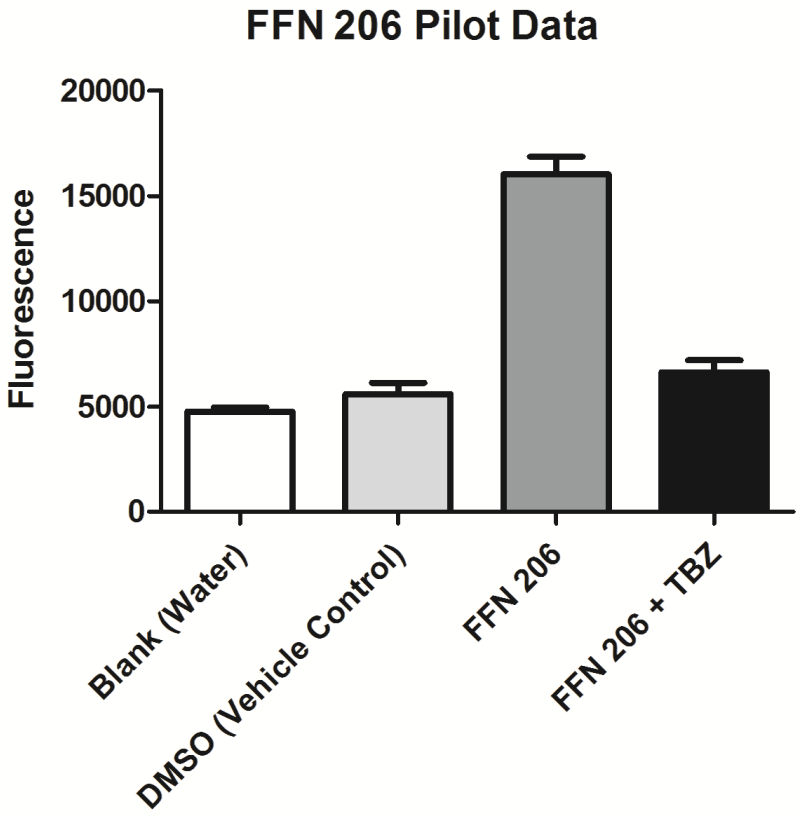

Figure 1. FFN206 Pilot Data

Initial proof of principle data for FFN 206 feasibility, bars indicate Standard Error of the Mean (SEM). FFFN 206 specific fluorescence can be detected, and is tetrabenazine (TBZ) sensitive. FFN 206 fluorescence is significantly different than FFN 206 fluorescence suppressed by TBZ. ($p < 0.01$). No significant difference between vehicle control and TBZ suppressed fluorescence. $Z' = 0.278$ (not suitable for high through put screening).

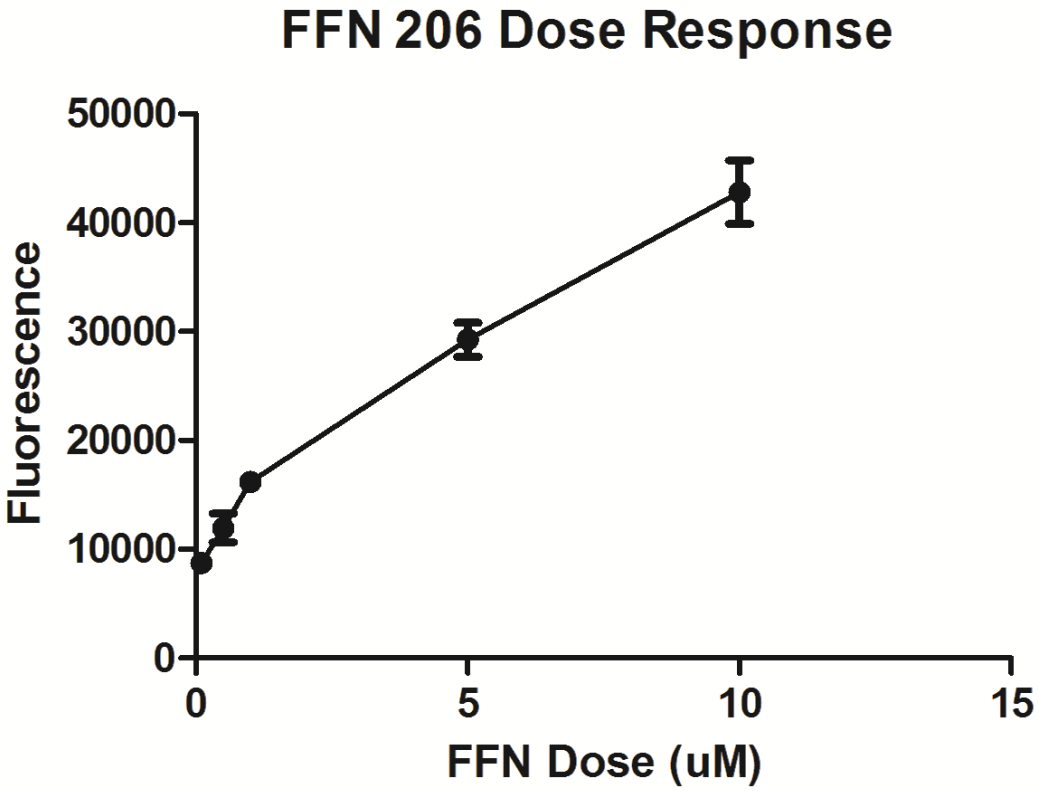

Figure 2. FFN 206 Dose Response.

FFN 206 fluorescence is dose-dependent.

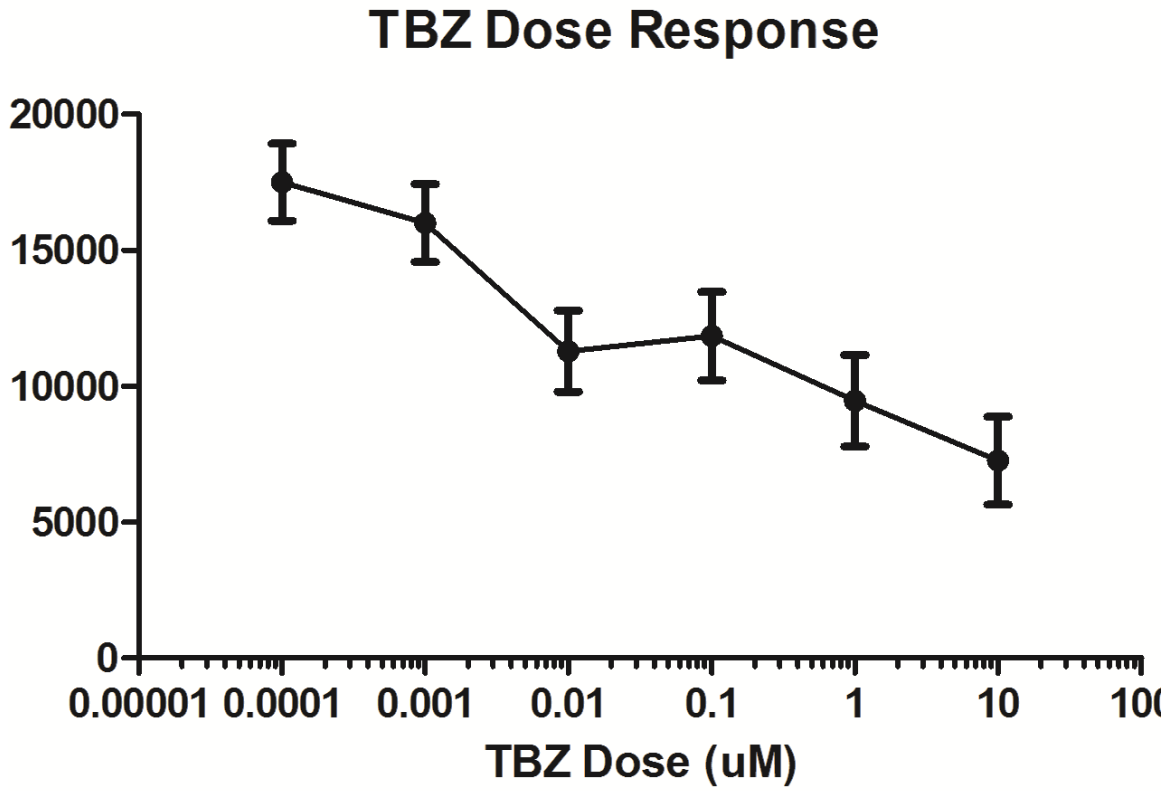

Figure 3. TBZ Dose Response.

TBZ suppression of FFN 206 fluorescence is dose-dependent.

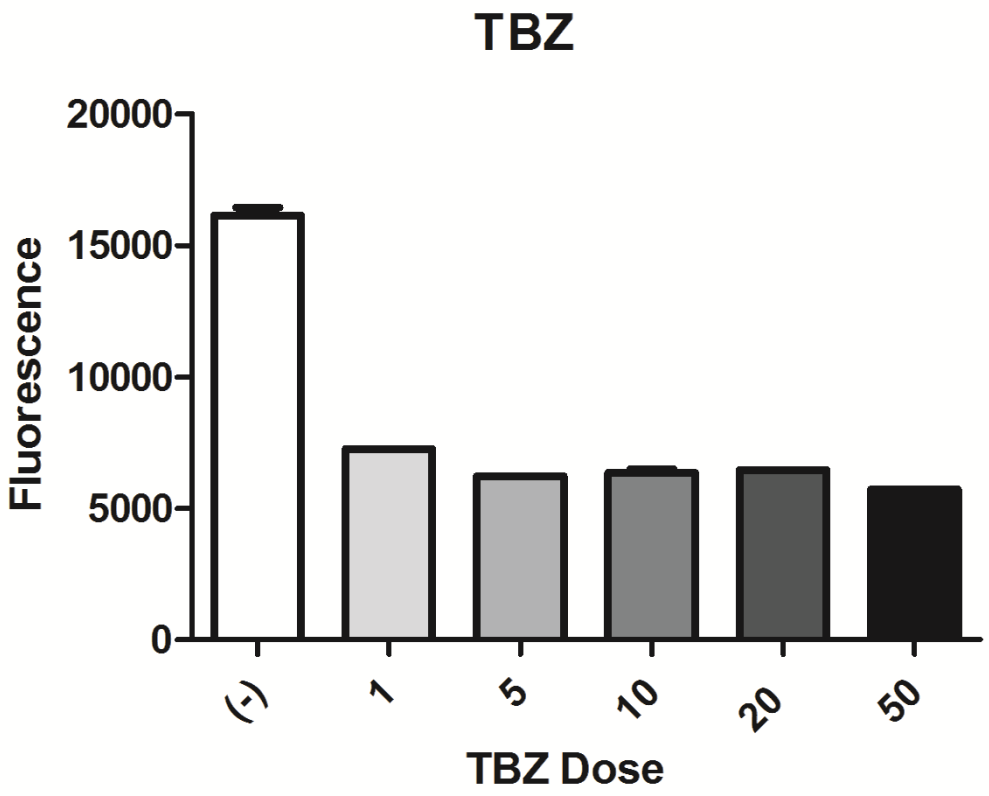

Figure 4. Selection of TBZ dose.

No significant different was found across a narrower range of TBZ doses. 10 uM was selected as starting dose for TBZ suppression.

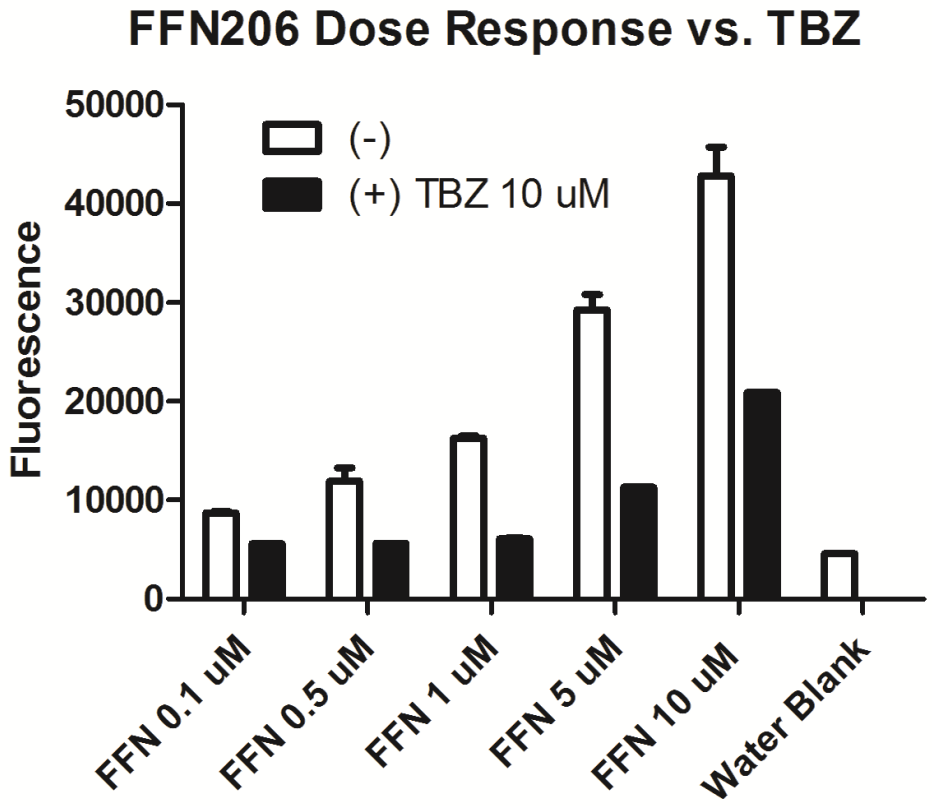

Figure 5. FFN 206 Dose Selection.

Broad range FFN 206 concentration was tested against selected concentration of 10 uM TBZ. For doses as high as 1 uM, FFN 206 is exquisitely TBZ sensitive. A midlevel dose of FFN 206 is chosen (below 10 uM) to ensure the assay has the dynamic range necessary to detect increases in VMAT function.

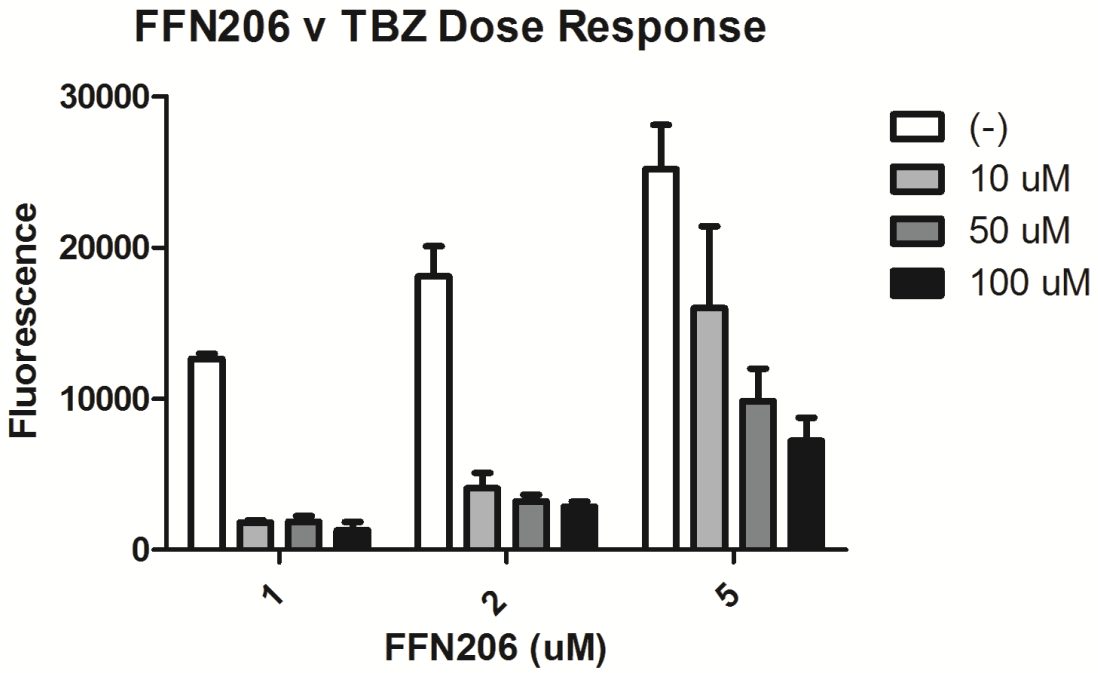

Figure 6. FFN 206 and TBZ dose interaction.

A narrow range of optimized FFN 206 concentrations was tested against a narrow range of optimized TBZ concentrations. Lower variability observed in lower doses of both FFN 206 and TBZ improves z factor analysis.

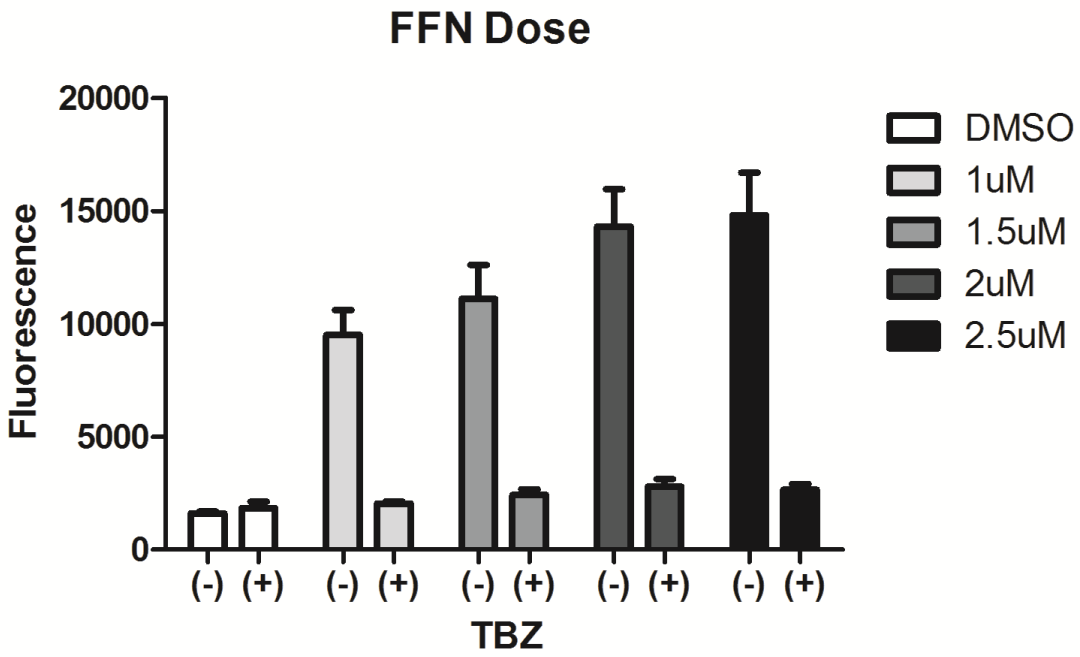

Figure 7. FFN 206 and TBZ dose interaction.

A narrower range of optimized FFN 206 concentrations was tested against 10 uM TBZ. 1 uM FFN 206 was selected based on z factor analysis and cost management.

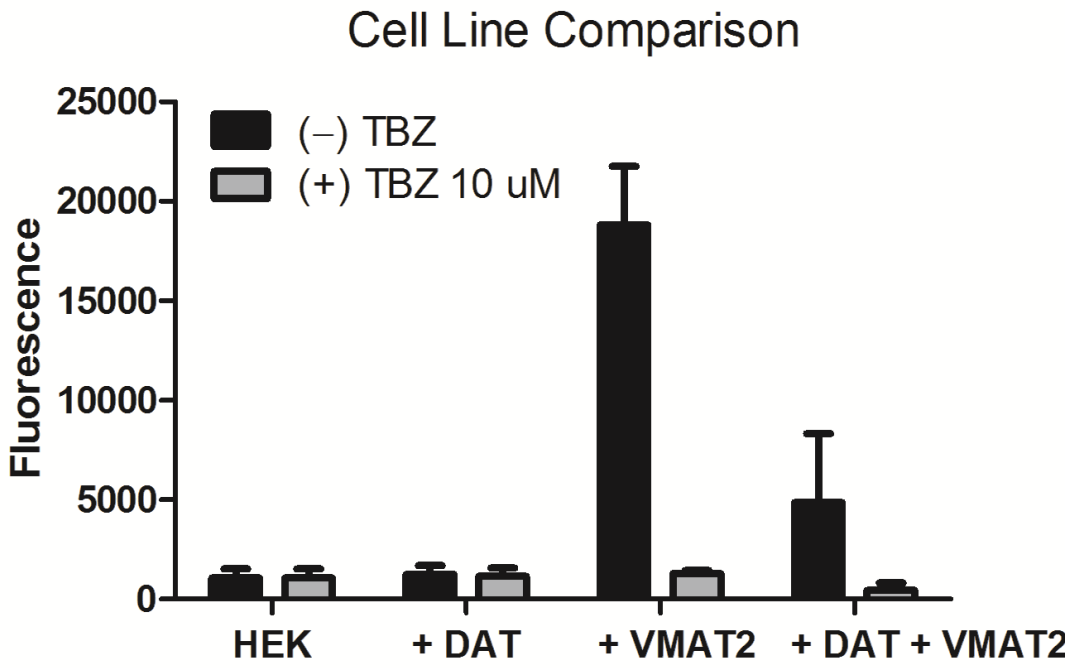

Figure 8. Cell Line Comparison.

Protocol was conducted on multiple cell lines. FFN 206 fluorescence was found to be VMAT specific and not DAT dependent for cell entry. Although putative drugs targeting VMAT may be DAT dependent for cell entry, further experiments were conducted in VMAT only cell line due to DAT/VMAT z factor below 0, therefore unsuitable for high through-put use. Lower fluorescence in this cell line is likely due to intrinsic factors of cell line and lower transfection efficiency for the double construct.

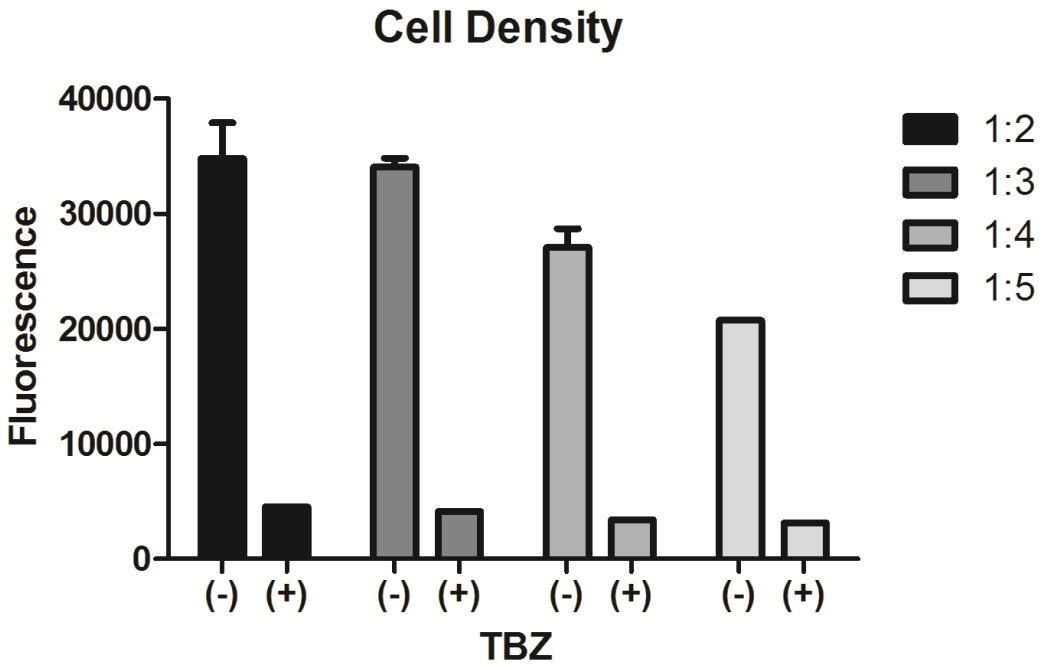

Figure 9. Cell Density

To determine if fluorescence scaled with cell density, cells were plated at multiple dilutions 24 hours before the assay. Fluorescence was found to scale with cell density. Cells at the highest density showed greater variability due to visible patches where cells lifted off the plates during multiple media changes and wash steps. Cells at ~90% were found to be best suited for assaying. Time between plating and assay was found to be far more flexible than final density at the time of assay, so when cells were not at 85-90% at the time of scheduled experiment, the experiment was rescheduled, rather than assaying sparse plates.

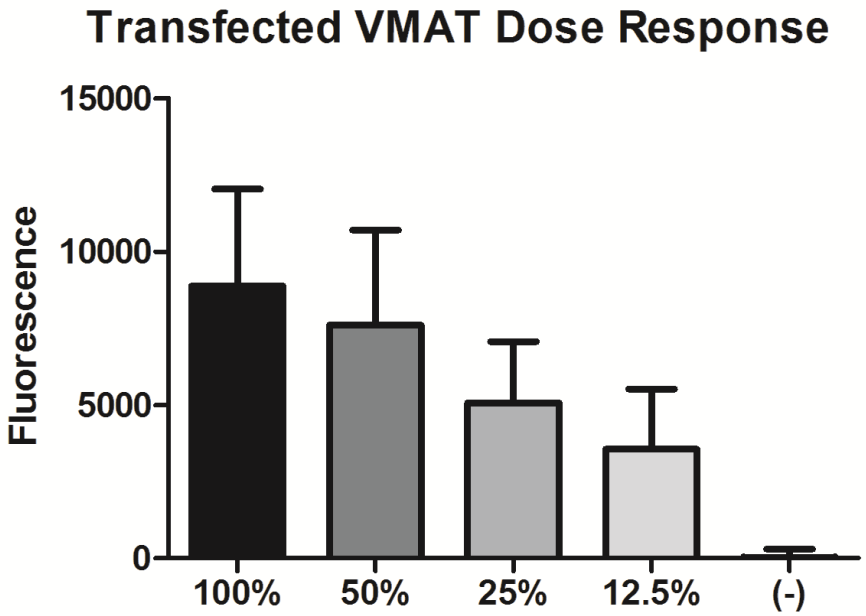

Figure 10. VMAT Dose Response

As another proxy to determine if FFN206 fluorescence scales with VMAT function, varying amounts of VMAT2 construct were transfected, beginning with the optimized transfection protocol, and decreasing by a factor of 2. As expected, FFN206 fluorescence scales with VMAT copy number.

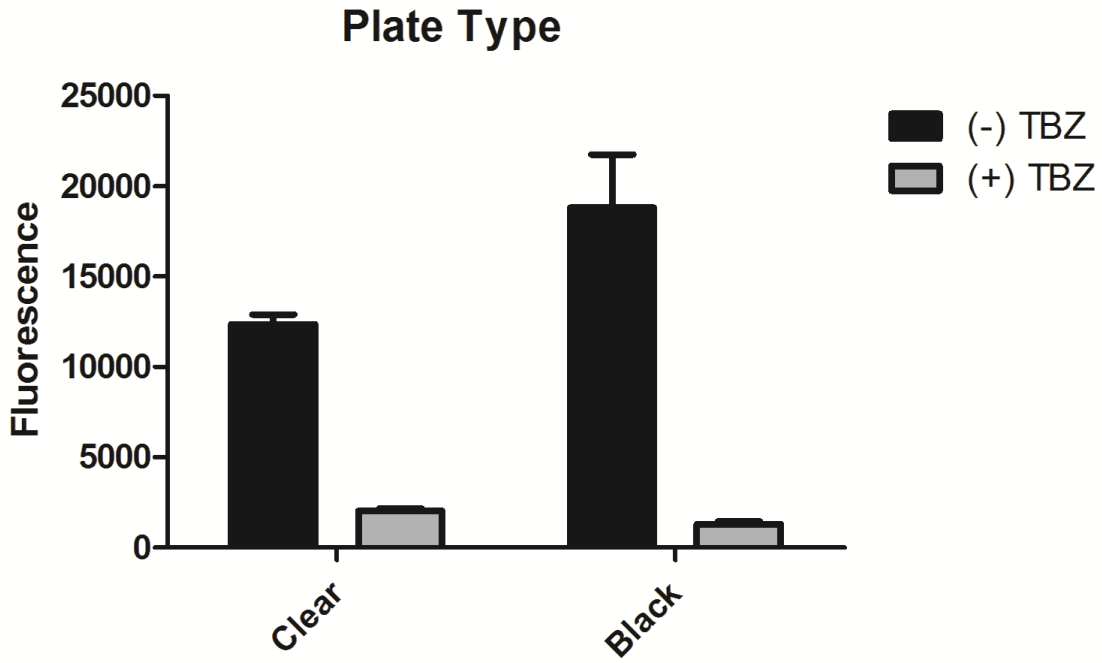

Figure 11. Plate type.

Clear walled plates were compared to black walled plates (both with clear bottoms). Data shown were normalized to water blanks. Black walls prevent overflow fluorescence between wells and increase the difference in fluorescence count between positive and negative controls.

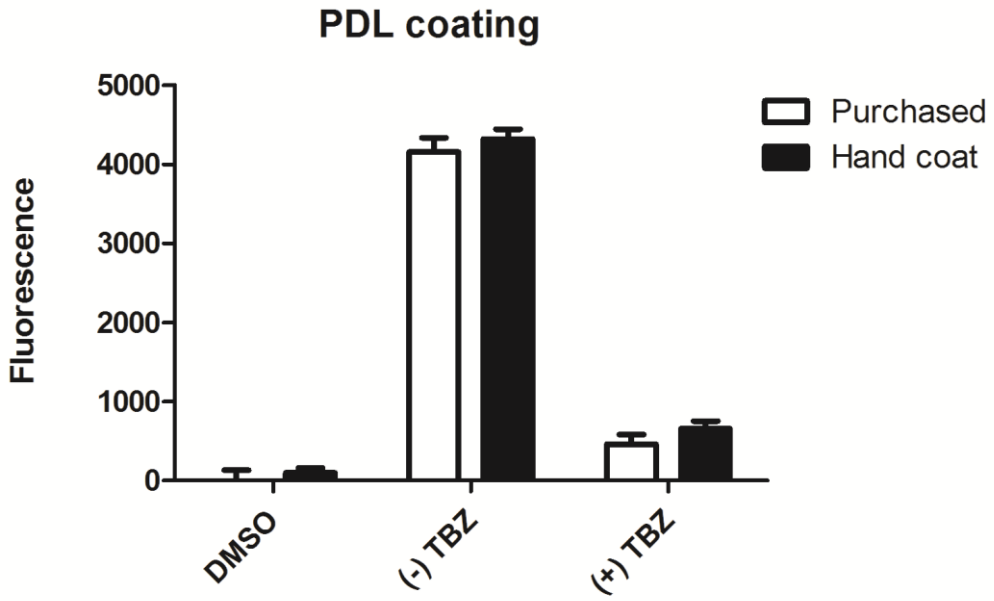

Figure 12. PDL coating

Protocol was conducted using plates purchased pre-coated with PDL and compared to coating plates in house with PDL as described in methods. Data shown is DMSO subtracted, to account for the difference in autofluorescence of the plate plastics. Hand coating was found to be both superior and more cost effective.

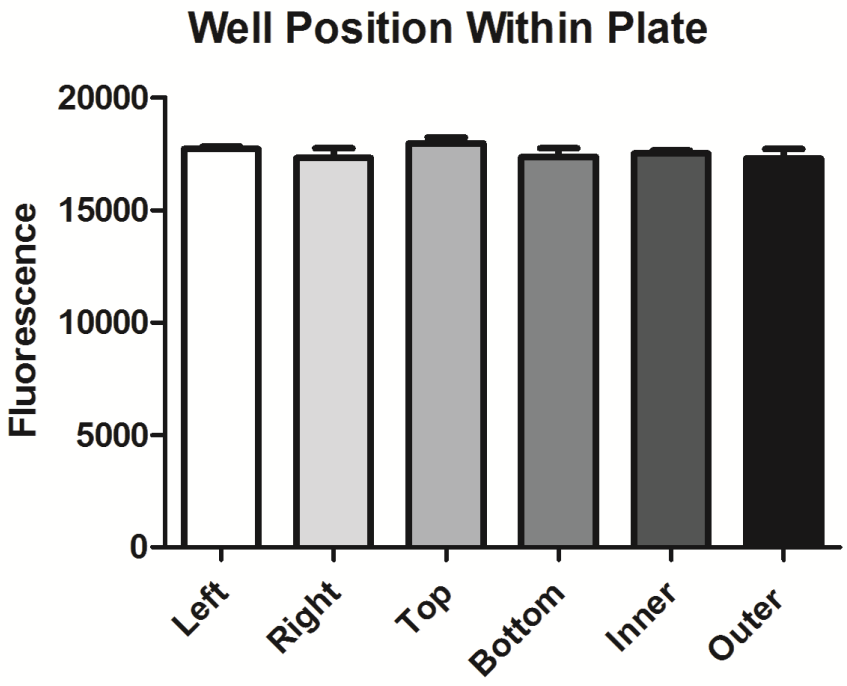

Figure 13. Well Position Within Plate.

Initial pilot experiments had shown a trend for higher reads on the left of the plate, and the inner wells of the plate. Cell plating technique was adjusted to ensure even pipetting into each well, with trituration to prevent cell settling; new multichannel pipettes were purchases to ensure even performance for each tip; and plate reader reading dimensions were adjusted to ensure no overlap with well reads until no significant difference was found between wells in different plate locations.

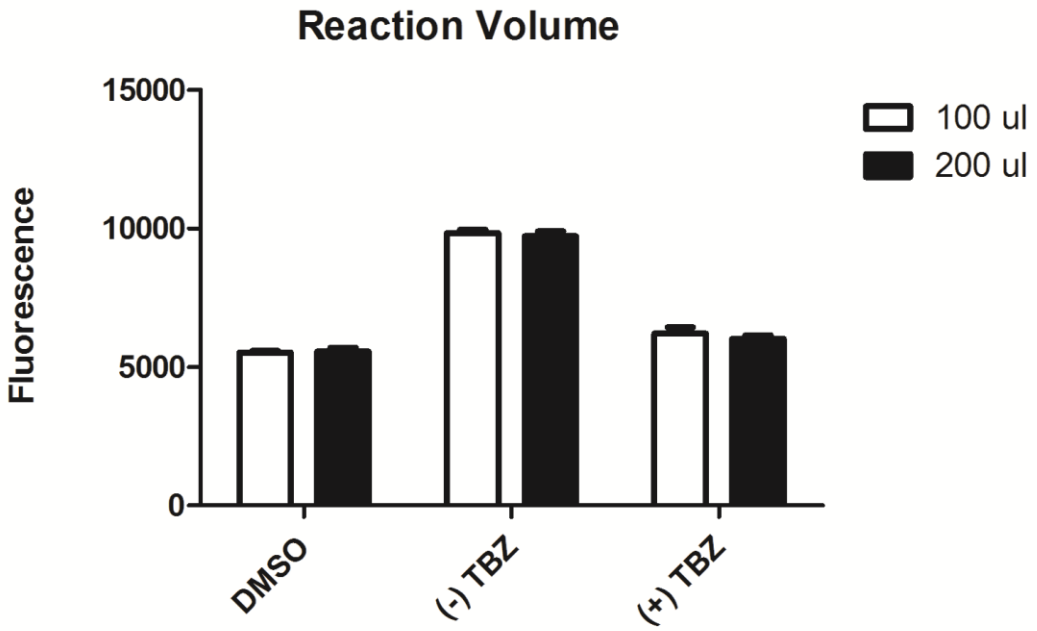

Figure 14. Reaction Volume Reduction.

Protocol was conducted in original volume and half volume to determine if smaller wells/ fewer reagents could be used without affecting the z factor. No significant difference was found between reaction volumes ($p = 0.63$). Protocol was then used with 100 µL total reaction volume.

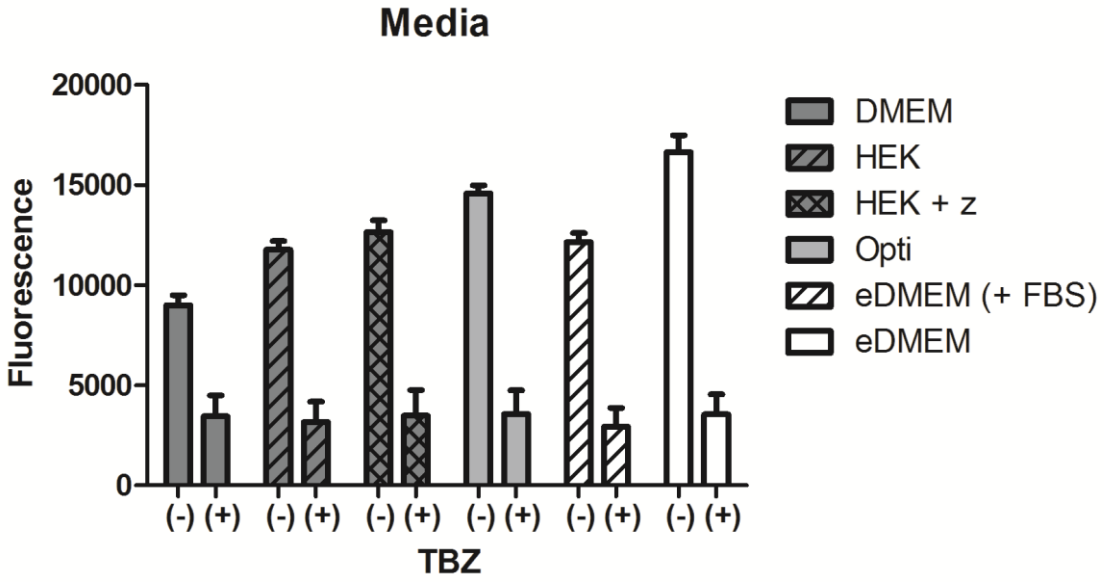

Figure 15. Media.

Protocol was tested with various media to determine which was most conducive for assay. Media varied by color due to the presence of phenol red (indicated by darker bar color), by the presence of FBS (indicated by hatching), and the presence of zeocin as selection antibiotic (indicated by cross hatching). eDMEM, as described in the methods section, was found to be the best choice for the assay.

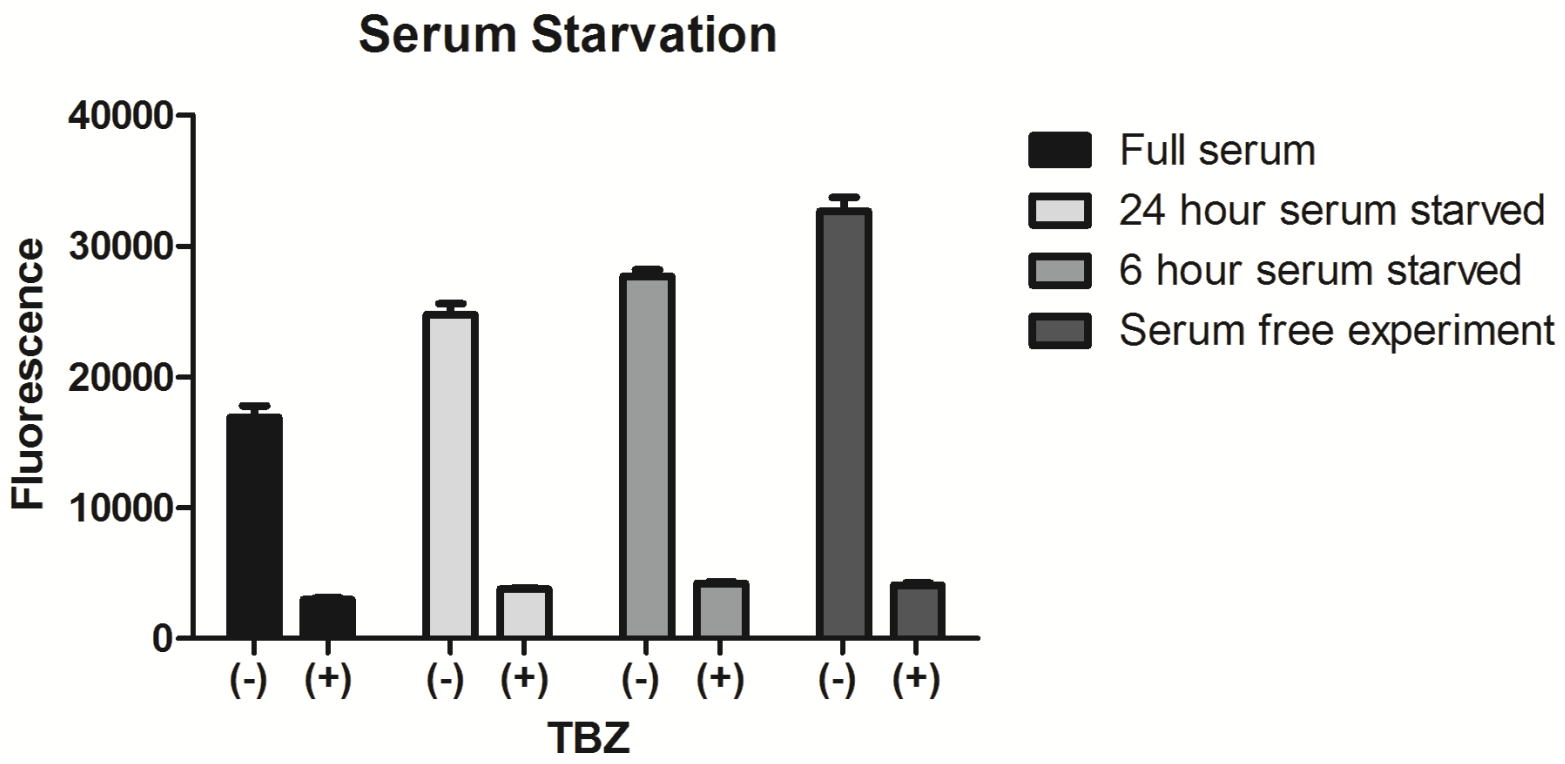

Figure 16. Serum Starvation.

To determine if the improved fluorescence in media without FBS was due to interference from FBS during the assay or cell function changes from short-term serum starvation, the protocol was conducted in full serum media, and with prior serum starvation of 0, 6, or 24 hours then assayed in serum-free experimental media. Results show that although removing FBS from the media improves assay results, additional serum starvation diminishes results, likely due to decreased cell proliferation or decreased packaging of FFN into vesicle compartments.

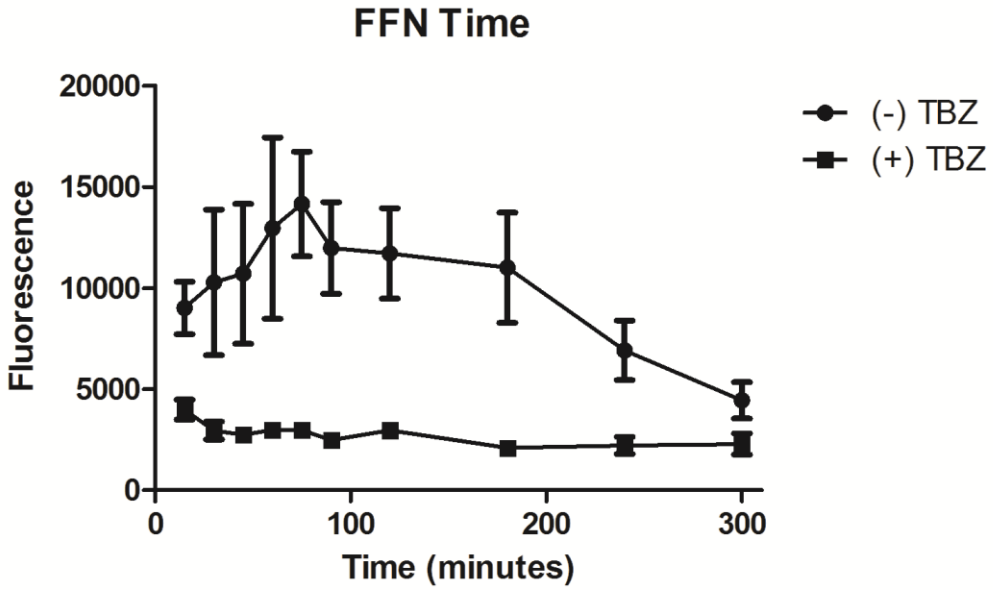

Figure 17. FFN Time.

To determine the ideal incubation time for FFN206, a time course was conducted. Fluorescence peaked at an incubation time of 75 minutes, which was selected for the optimized protocol. The relative stability of the data shows that while 75 minutes is ideal, for less sensitive tasks, 60-90 minutes may be chosen as a suitable incubation time.

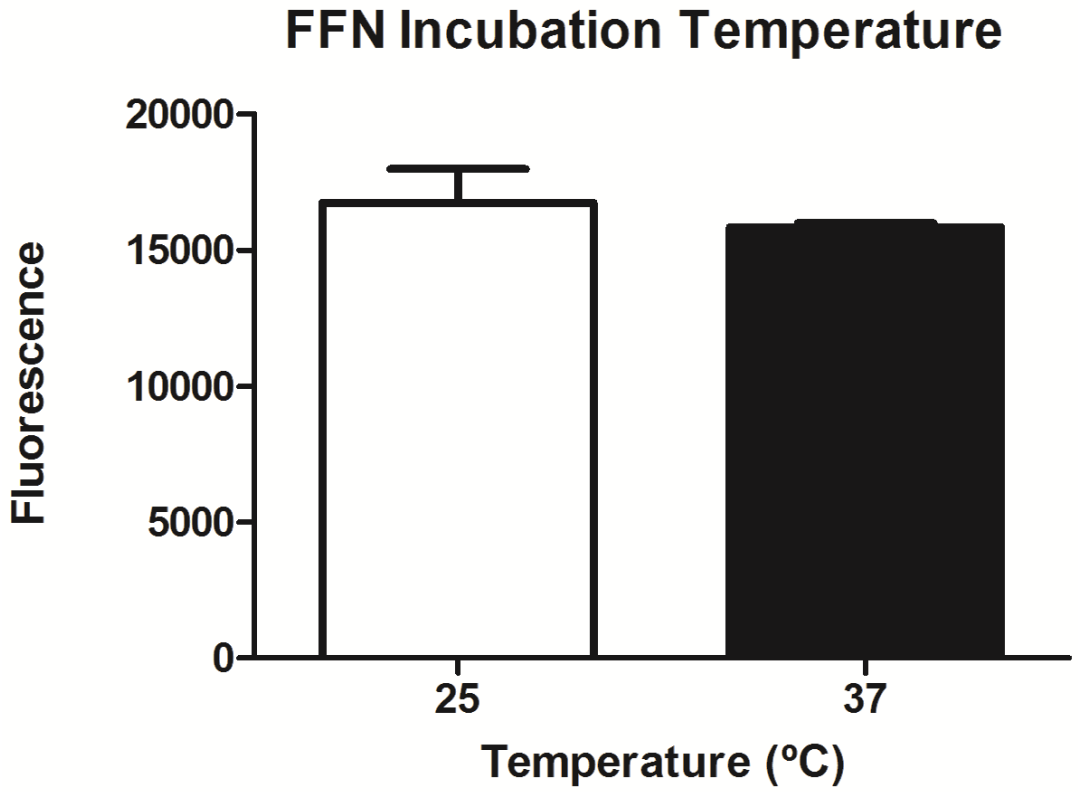

Figure 18. FFN Incubation Temperature.

Incubation at 37 ºC was compared to room temperature. Although 37 ºC is preferred for its smaller variability and physiological relevance, no significant difference was found between incubation temperatures, indicating that the assay will be robust to possible variations in temperature during plate handing in high throughput use.

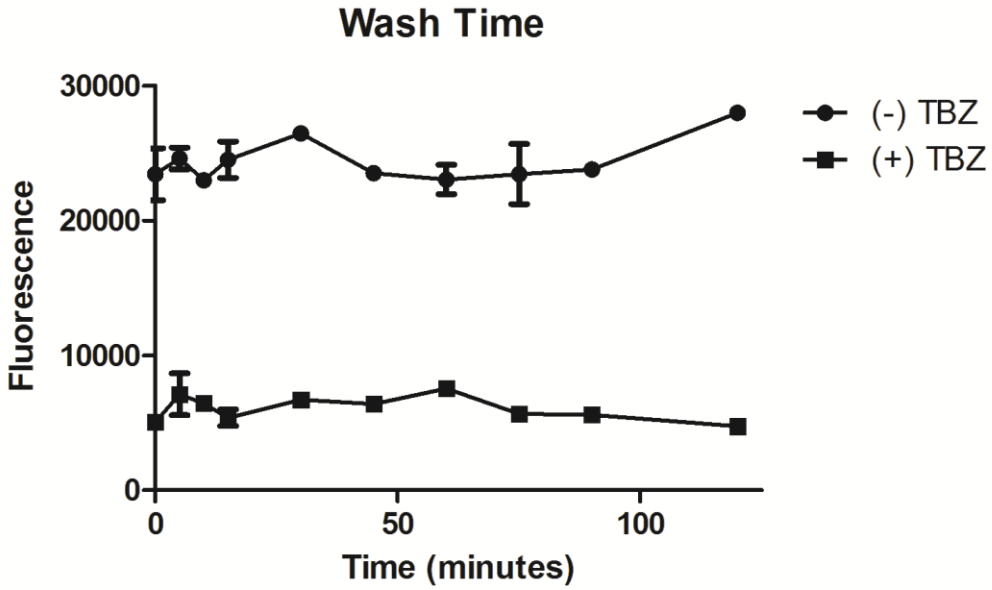

Figure 19. Wash Time.

To determine the stability of fluorescence, a time course of wash time (time between washing to remove fluorophore and reading the plate in the plate reader) was conducted. No significant degradation was observed out to 2 hours. Although plates were read immediately after washing when trials were conducted by hand, the stability of the fluorophore makes this assay well-suited for high throughput screens where delays may be introduced by the logistics of handling large numbers of plates.

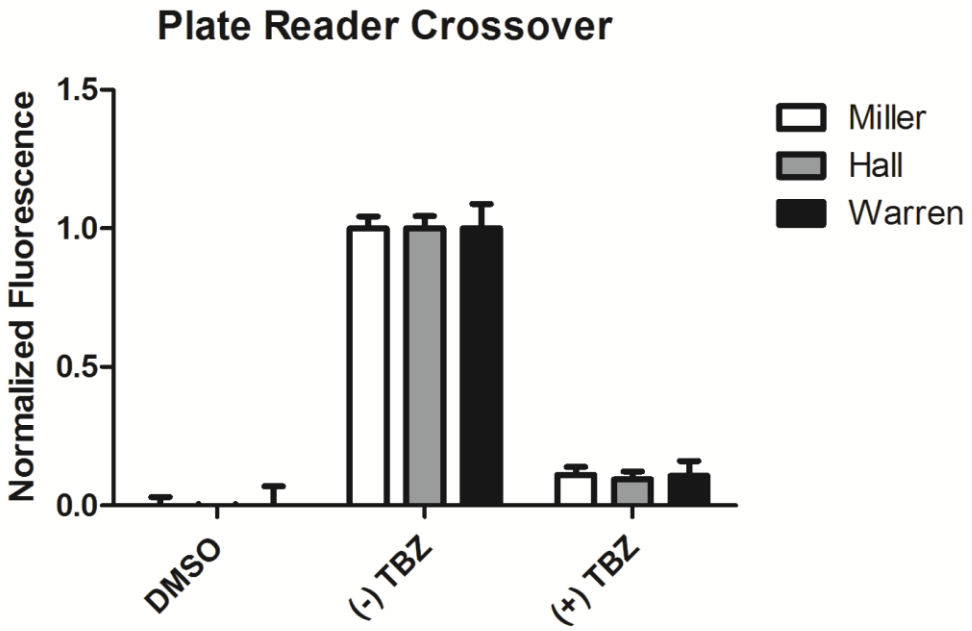

Figure 20. Plate Reader Comparison.

To investigate the robustness and reproducibility of the protocol, plates were read on three different plate reader brands, in three different laboratories. Once normalized by range, no significant difference was found between results from different plate readers, showing the consistency of this protocol.

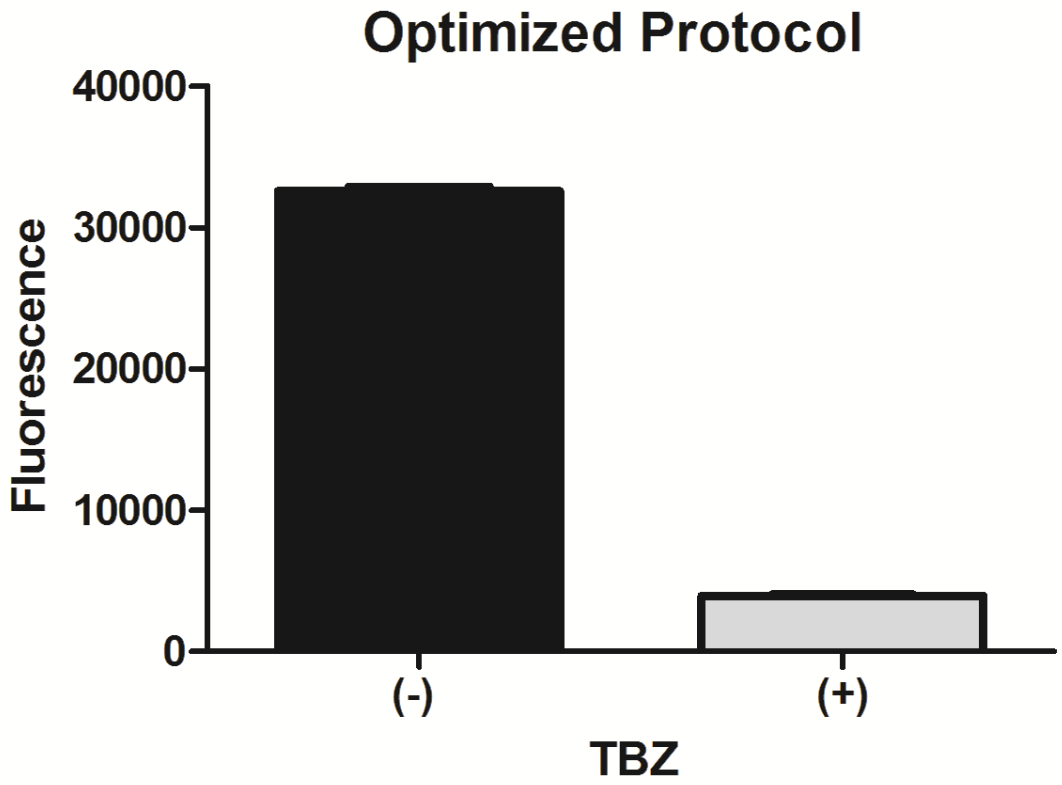

Figure 21. Optimized Protocol.

After optimizing the protocol, the optimized z' was consistently > 0.9. Shown here, z = 0.947.

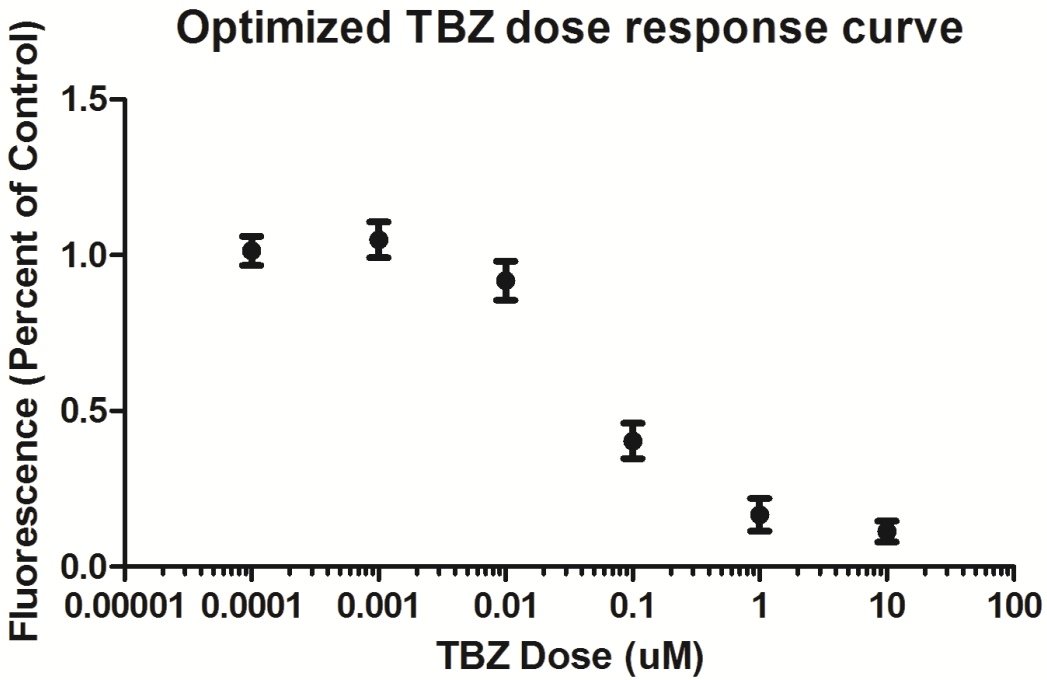

Figure 22. Optimized TBZ dose response curve.

The optimized assay was used to create dose response curves (TBZ shown here as an example) to demonstrate the utility of the assay for evaluating the effect of pharmacological compounds on VMAT activity. Fluorescence is shown here as percentage of uninhibited VMAT activity.

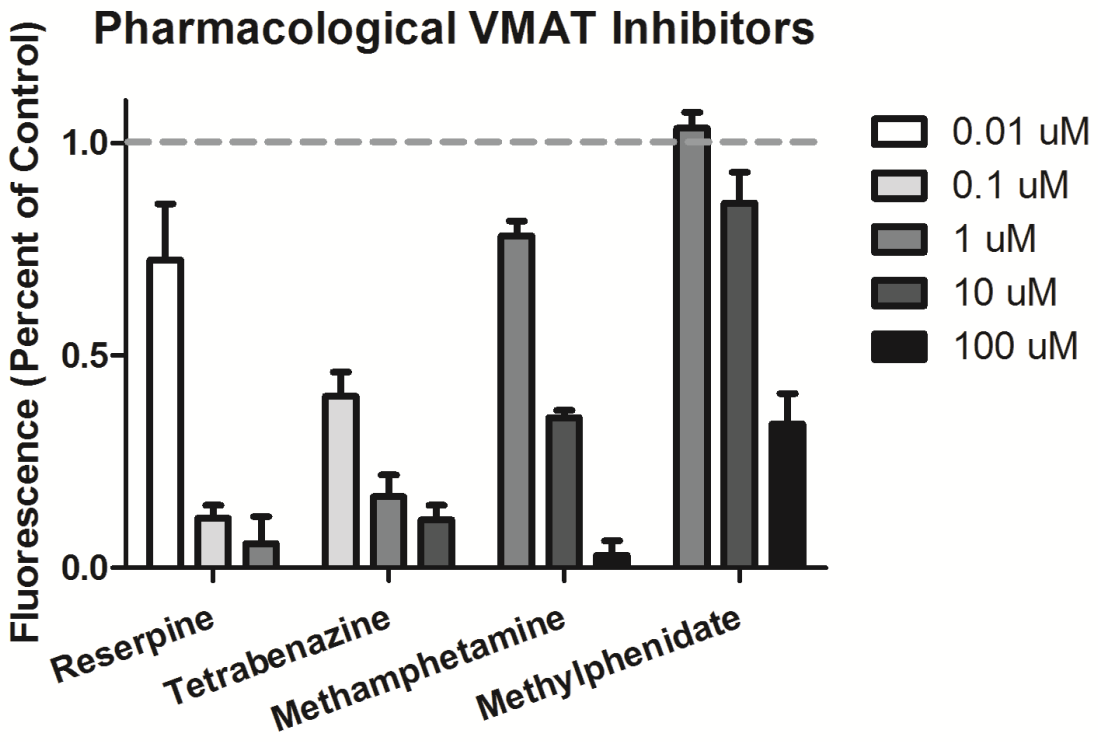

Figure 23. Pharmacological VMAT Inhibitors.

The optimized assay was used to test a variety of pharmacological VMAT inhibitors to demonstrate the utility of the assay for evaluating the effect of pharmacological compounds on VMAT activity. Relevant dosages of four known VMAT inhibitors are shown here as percentage of uninhibited VMAT activity (marked with dashed line).

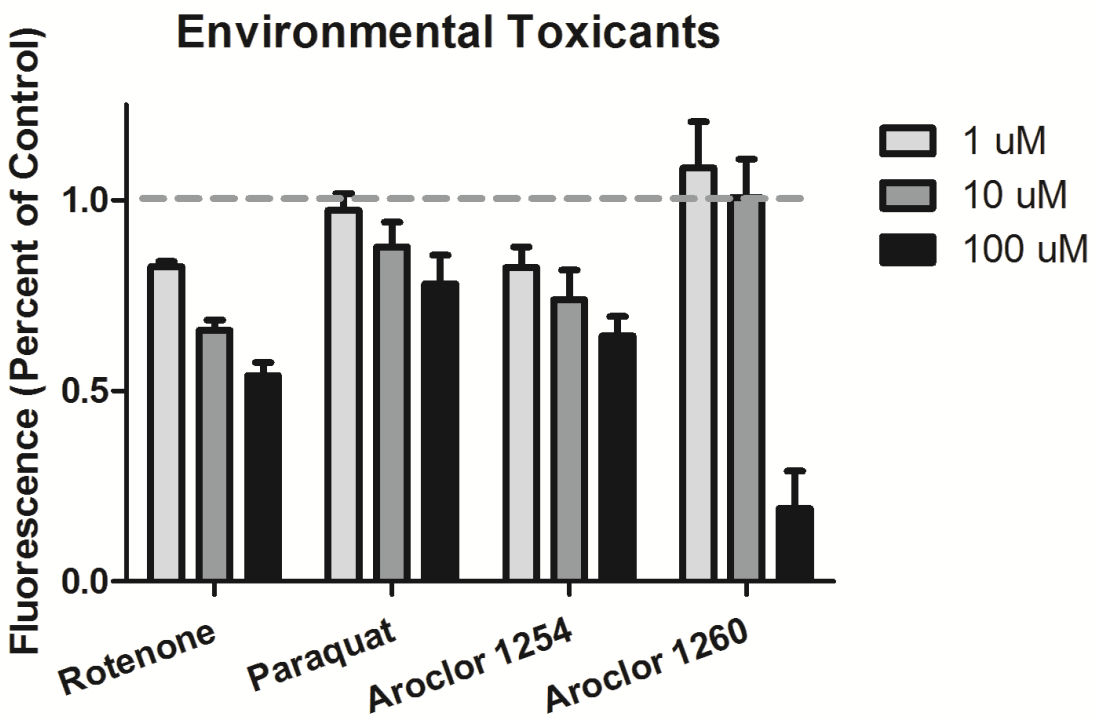

Figure 24. Environmental Toxicants.

The optimized assay was used to test a variety of environmental toxicants of interest due to association with Parkinson's disease risk. This demonstrates the utility of the assay for evaluating the effect of environmental toxicants on VMAT activity. Relevant dosages of four environmental toxicants are shown here as percentage of uninhibited VMAT activity (marked with dashed line).